CHEMPHYSCHEM

DOI: 10.1002/cphc.200800538

Direct Electrodeposition of Porous Gold Nanowire Arrays for Biosensing Applications

Xinyi Zhang,*[a] Dan Li,[a] Laure Bourgeois,[b] Huanting Wang,[a] and Paul A. Webley*[a]

We report the fabrication of porous gold nanowire arrays by means of a one-step electrodeposition method utilizing nanochannel alumina templates. The microstructure of gold nanowires depends strongly on the current density. The formation of porous gold nanowires is attributed to disperse crystallization under conditions of low nucleation rate. Interfacial electron transport through the porous gold nanowires is studied by electrochemical impedance spectroscopy. Cyclic voltammetric studies on the porous gold nanowire arrays reveal a low-potential electrocatalytic response towards hydrogen peroxide. The properties of the glucose oxidase modified porous gold nanowire array electrode are elucidated and compared with those of nonporous enzyme electrodes. The glucose oxidase modified porous gold nanowire-array electrode is shown to be an excellent electrochemical biosensor for the detection of glucose.

1. Introduction

One-dimensional (1D) nanostructures have stimulated tremendous interest due to their importance in basic scientific research and potential technological applications.[1,2] Porous nanowires are a special type of 1D nanomaterials that combine porous nanostructure with 1D geometry.[3,4] The extremely high surface-to-volume ratios associated with these nanostructures make their properties extremely sensitive to species adsorbed on surfaces and result in excellent sensitivity and selectivity. With their porosity and high specific surface area, porous nanowires have shown considerable promise in catalysis, separation, hydrogen adsorption, and chemical sensors.[5–8] Moreover, the presence of void space in nanowires can allow the incorporation of multiple components to form hybrid nanocomposites, and such nanostructures are expected to have novel characteristics that combine the features of two or more distinct classes of materials. Among the strategies for preparing 1D nanostructures, a simple and versatile approach is deposition of the desired material into an alumina template with porous nanochannels.[9–14] Gold has been widely used as an electrode material because of its high chemical and thermal stability, excellent electric conductivity, and biocompatibility.[15–20] Ji and Searson demonstrated the preparation of porous gold nanowires based on membrane-template electrocodeposition of a single-phase, two-component alloy followed by selective dissolution of the less noble component.[21] More recently, steplike porous gold nanowires of different shapes were prepared by sequentially depositing alloy segments with different gold/silver ratios and de-alloying the silver component.[22]

The area of biosensors, particularly enzyme-based electrochemical sensors, has received great attention over the past forty years. Considerable efforts have been made to obtain biosensors for fast and reliable quantification of compounds of biomedical interest, particularly glucose.[23,24] Electrochemical biosensors for glucose based on the enzymatic oxidation mediated by glucose oxidase (GOx) have generated considerable interest.[25–28] Gold nanowires are ideal nanoelectrodes for miniaturized electrochemical sensors. In this article, we demonstrate that porous gold nanowire arrays can be fabricated by means of a one-step electrodeposition method utilizing nanochannel alumina (NCA) templates. A glucose biosensor based on a porous gold nanowire array modified by GOx was fabricated and exhibited excellent bioactivity toward glucose.

2. Results and Discussion

Figure 1a shows SEM images of the gold nanowire arrays, which result from carefully etching away the alumina. The average pore diameter and thickness of the NCA template are 65 nm and 2 μm, respectivley. The gold nanowires replicate the pore sizes, shapes, and positions. The fine structure of the nanowires is clearly visible in the high-magnification SEM image (Figure 1b). The dispersed nanosized protrusions (or particles) that can be distinctly observed on the surfaces of the nanowires reveal that the gold nanowires are formed by inhomogeneous accumulation of nanoparticles. The microstructure of the gold nanowires was further investigated by TEM. Figure 2a shows a bright-field image of the gold nanowires after completely dissolving the NCA template. Some light spots that can be seen on the gold nanowires reveal the existence of pores in the nanowires. Figure 2b shows a high-magnification image of a single gold nanowire, and the pore structure of the

[a] *Dr. X. Y. Zhang, Dr. D. Li, Dr. H. T. Wang, Dr. P. A. Webley*
Department of Chemical Engineering
Monash University, Clayton, VIC3800 (Australia)
Fax: (+61) 3-99055686
E-mail: xinyi.zhang@eng.monash.edu.au
Paul.webley@eng.monash.edu.au

[b] *Dr. L. Bourgeois*
Monash Centre for Electron Microscopy, Monash University
Clayton, VIC3800 (Australia)

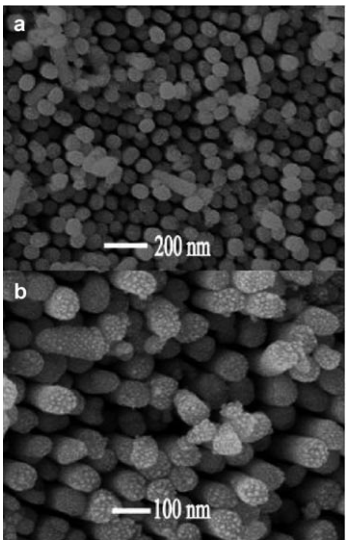

Figure 1. SEM images of the top view of the Au nanowire arrays prepared within an NCA template with 65 nm pore diameter: a) low and b) high magnification.

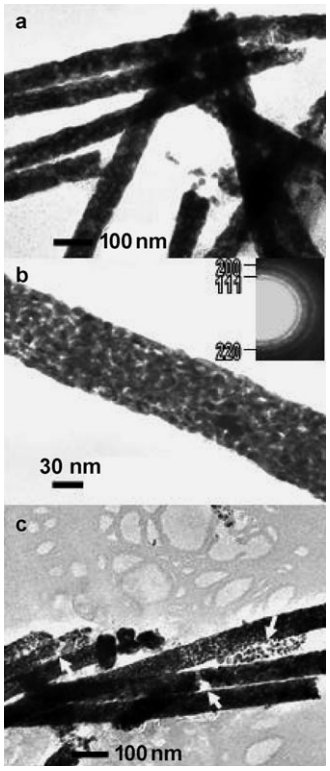

Figure 2. a) Bright-field TEM image of the Au nanowires. b) High-magnification bright-field TEM image of a single Au nanowire and its corresponding electron diffraction pattern. c) Bright-field TEM image of broken Au nanowires and Au nanoparticles resulting from disintegration of the Au nanowires.

gold nanowires can be unmistakably identified. The inset in Figure 2b shows a corresponding electron diffraction pattern, which can be indexed as face-centered cubic gold. These gold nanowires have unique characteristics: they consist of assembled nanoparticles with sizes ranging from several nanometers to about 10 nm. The loose packing of these nanoparticles results in the porous structure of the nanowires. As indicated in Figure 2c, these gold nanowires are rather friable and easy to be broken or disintegrated into particles, that is, the intercrystalline bonds in the porous nanostructures are weak.

Porous nanowires have been fabricated within templates by electrodeposition of a single-phase, two-component alloy followed by selective dissolution of the less noble component.[21,22] However, there is no report on the direct electrodeposition of porous nanowires. An explanation of the growth mechanism of porous nanowires must remain speculative. In galvanostatic electrodeposition, the critical energy for nucleation is determined by the free energy of the surface of a nucleus and the driving force (current density). The higher the current density, the easier it is for nucleation to take place.

Figure 3 shows the overpotential versus time curve of the gold deposition within the NCA templates at different current densities. Gold deposition is strongly dependent on current

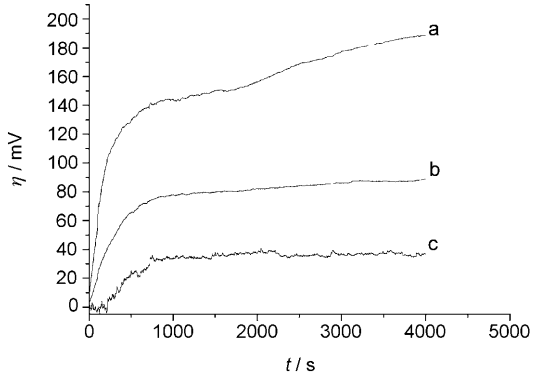

Figure 3. Overpotential–time curves of electrodeposition within an NCA template with 65 nm diameter at different current densities: a) 200, b) 50, and c) 10 $\mu A\,cm^{-2}$.

density. The initial potential shift corresponds to nucleation and growth of Au deposits on the Au film substrate. At this stage, nucleation and growth of Au deposits take place on the existing Au film. The electrodeposition is base-oriented, and the microstructure of the Au deposits is an extension of the substrate. As shown in Figure 3, the initial depositions are approximately exponential. As the concentration of Au ions decreases, the diffusion overpotential of the cathode increases promptly to keep the constant current during this period. The overpotential shift increases with increasing current density. Then the structural change from base-oriented deposition to field-oriented texture is accompanied by an increase of overpotential, which corresponds to the crystallization overpotential that characterizes this transition.[29] At high current density, the polarization increases with time (Figure 3a). High overpotential and high growth rate result in compact polycrystalline nanowires with oriented texture.[30] At medium current density, the overpotential does not vary sensitively with duration of electrodeposition after the transition period, and it approaches a stationary value (Figure 3b). In this case, the deposition process approaches an equilibrium state, and oriented single-crys-

talline nanowires with smooth surface can be obtained.[31] At low current density, the overpotential shift is even smaller and polarization instability (potential oscillation) occurs (Figure 3c). In this situation, nucleation becomes difficult and slow, and the number of nuclei decreases because insufficient crystallization energy is supplied. Hence, these nuclei are selectively deposited on the cathode surface instead of covering the whole surface to reduce the energy of nucleation, and protrusions form at sites where metal ion discharge is concentrated. The protrusions on the cathode would then play an important part in the formation of porous deposits. The protrusions on the cathode surface make disperse crystallization easier by attaching nuclei of adatoms and offering sites of maximal current density.[32,33] It can be assumed that the concentration polarization and electrochemical polarization at these sites are smaller than in other regions of the cathode. Therefore, they are sites of preferential crystallization of the gold deposit. In other regions, where gold ions are deficient, no significant discharge occurs and thus no deposition takes places. The potential oscillation during electrodeposition also reveals nonuniform distribution of current density and inhomogeneous deposition. Repeated nucleation and growth of particles is especially biased towards higher electric field along the nanochannels, and thus a less tight packing is realized. This results in the formation of porous gold nanowires.

Electrochemical impedance spectroscopy (EIS) is a rapidly developing electrochemical technique for the characterization of biomaterial-functionalized electrodes and biocatalytic transformations at electrodes surfaces, and specifically for the transduction of biosensing events at electrodes.[34,35] To characterize the interfacial properties of porous gold nanowire array electrodes, Nyquist impedance measurements were performed in 0.1 M phosphate buffer solution (PBS, pH 7.0) by using 10 mM $[Fe(CN)_6]^{3-/4-}$ as redox probe. Figure 4 shows the Nyquist impedance plot of porous and nonporous gold nanowire-array electrodes before (i, ii) and after (iii, v) GOx immobilization. In general, the shapes of the impedance spectra mainly include the linear parts, that is, the impedance of these gold nanowire-array electrodes is mainly controlled by diffusion of the redox probe due to very fast electron-transfer processes. However, significant differences in the impedance spectra can be observed in the high-frequency regions, which correspond to the electron-transfer-limited process. The impedance of the porous gold nanowire-array electrode follows the linear line, whereas the impedance spectrum of nonporous gold nanowire-array electrodes includes a semicircle region at high frequencies. The spectrum of the porous gold nanowire arrays exhibits the characteristic features of porous electrodes.[36,37] At high frequencies, the electrode admittance is great, and thus the alternating current signal is damped within a short distance.[38] Therefore, a straight line results in the Nyquist plot. After GOx immobilization, impedance spectra with larger semicircular regions can be obtained from both porous and nonporous gold nanowire-array electrodes. The increase in the charge-transfer resistance R_{ct} reveals the formation of a glucose oxidase layer adsorbed on the electrode surface, which exhibits a barrier effect to the electron-transfer kinetics. As can be seen in the

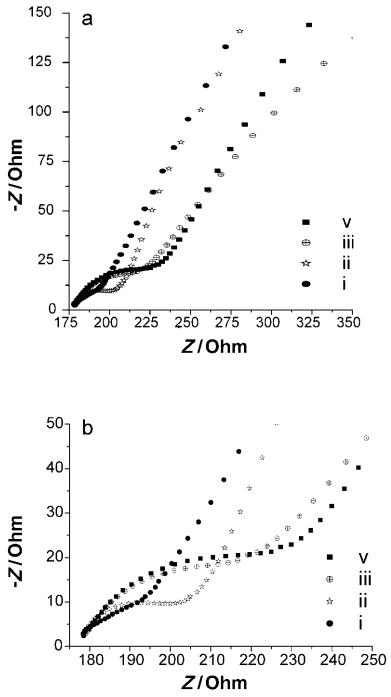

Figure 4. a) Nyquist plot in 0.1 M phosphate buffer solution (pH 7.0) in the presence of 1 mM $[Fe(CN)_6]^{3-/4-}$ for i) porous gold nanowire array, ii) nonporous gold nanowire array, iii) GOx-modified nonporous gold nanowire array, and v) GOx-modified porous gold nanowire array. b) Enlarged high-frequency region of the Nyquist plot.

spectra, the R_{ct} value for the GOx-modified porous gold electrode is higher than that of the GOx-modified nonporous gold electrode, that is, the porous gold nanowires provide excellent sites to adsorb GOx and result in more compact layer than the nonporous electrodes.

Gold electrodes have been widely used for the detection of H_2O_2 and the fabrication the oxidase-based biosensors. Figure 5 shows cyclic voltammograms (CVs) of porous gold nanowires in 0.1 M PBS (pH 7) at a scan rate of 10 mV s^{-1} in the absence and presence of 0.5 mM H_2O_2. The electrode exhibits the expected steady-state current response in the absence of H_2O_2. The anodic current increases during the forward sweep, and a peak current is observed at 0.38 V, which is due to the formation of less active gold oxides. The cathode current

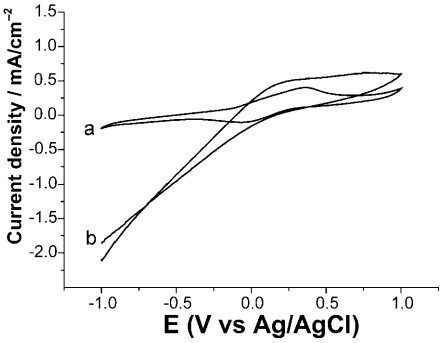

Figure 5. Cyclic voltammograms of porous gold nanowire array electrodes in the absence (a) and presence (b) of 0.5 mM H_2O_2.

peaks can be observed at −0.01 V during the backward sweep, which can be attributed to reduction of the gold oxide formed during the positive-going sweep.[39] Redox peaks of this kind usually appear on gold nanoelectrodes, such as nanoporous gold film[40] or gold nanowire arrays,[41] because the nanoelectrodes are easier to oxidize than smooth electrodes due to their high electrochemical activities. When H_2O_2 was added to the solution, an obvious enhancement in both cathodic and anodic current could be observed, which is due to electrocatalytic reduction and oxidization of H_2O_2. Note that the remarkable reduction current can be achieved at as low as 0 V, which is much lower than the values on the conventional Au electrode. It can be inferred that the fast interfacial electron transfer on the porous gold nanoelectrodes offers a decreased overpotential and increased response current to hydrogen peroxide.

The overall oxidation reaction of glucose at a GOx-based biosensor electrode is given by Equation (1).[42]

$$\text{Glucose} + O_2 \xrightarrow{\text{GOx}} \text{Gluconic acid} + H_2O_2 \quad (1)$$

Thus, glucose can be determined from the consumption of oxygen and the products of the enzyme reaction: gluconic acid and H_2O_2. Glucose concentration can be determined by an amperometric method by measuring the cathodic current of enzymatically liberated H_2O_2 in the enzyme electrode.[43] This amperometric method allows measurement of the cathodic current of resultant H_2O_2 at low potential, and the responses of common interference species (such as uric acid, ascorbic acid) can be minimized. The biocatalytic activity of the GOx-modified porous gold nanowire arrays was measured in PBS at a constant potential of −0.1 V. Figure 6 illustrates typical amperometric responses to successive concentration increments of 1 mM glucose at the GOx-modified porous gold nanowire-array electrode. The lower left inset shows the amperometric responses of the enzyme electrode to successive concentration increments of 50 μM of glucose. The rapid response (ca. 5 s) to the changes in glucose concentrations indicates excellent electrocatalytic behavior of the biosensor nanoelectrode array. The cathodic current increases stepwise with injection of glucose. The catalytic current is linearly proportional to glucose concentration from 5×10^{-5} to 2×10^{-3} M with a correlation coefficient of 0.99906. From the calibration curve a linear relationship with regression equation of $I(\mu A) = 0.03235 + 1.95848\,C(\text{mM})$ can be obtained (upper right inset, Figure 6). The sensitivity of the GOx-modified porous gold nanowire-array electrode is about 15.6 $\mu A\,cm^{-2}\,mM^{-1}$, which is higher than 5.11 and and similar to 15.1 $\mu A\,cm^{-2}\,mM^{-1}$ for GOx-modified gold electrodes based on layer-by-layer covalent attachment.[19,44] The detection limit (dl) was calculated as $dl = 3\sigma_b/m$, where σ_b is the standard deviation of the background current, and m the slope of the linear part of the calibration curve.[45] A detection limit of 4.6×10^{-5} M can be obtained, which is in the typical range of detection limits of GOx-based biosensors.[19,27,44,46] The effect of ascorbic acid was investigated by measuring the amperometric response toward 0.5 mM ascorbic acid, and the absence of observable interference at −0.1 V suggests that ascorbic acid is not electrochemically active at this potential. This result is consistent with those of previous studies.[27,44] Properties of the glucose-oxidase-modified nonporous gold nanowire array electrode were also studied. Figure 7 illustrates amperometric current responses of the GOx-modified solid gold nanowire-array electrode to successive concentration increments of 1 mM of glucose. The sensitivity and response time for the immobilized enzyme electrode are about 8.76 $\mu A\,cm^{-2}\,mM^{-1}$ and 7 s, respectively. The stabilities of both porous and nonporous GOx-modified gold nanoelectrodes were assessed by examining their amperometric current responses to 5 mM glucose each day. After 7 d of measurement, the responses of the porous and nonporous enzyme electrodes remained at about 85 and 74% of the original values, respectively. The porous enzyme electrode shows better performance than the nonporous enzyme electrode. It can be inferred that the void spaces of porous gold nanowires provide ideal sites to adsorb GOx and maintain its activity. Hence, the porous gold nanowire-

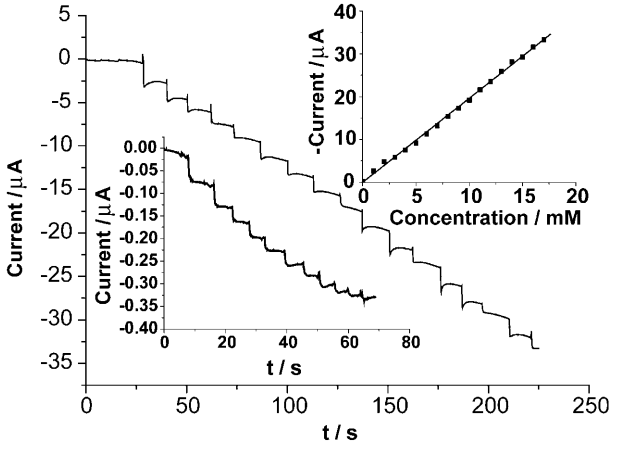

Figure 6. Response of the current–time curve of the GOx-modified porous gold nanowire-array electrode to successive additions of 1 mM glucose at −0.1 V in 0.1 M PBS. The lower left inset shows the current–time curve of the GOx-modified porous gold nanowire-array electrode to successive additions of 50 μM glucose. The upper right inset shows the calibration curve of the GOx-modified porous gold nanowire-array electrode toward glucose.

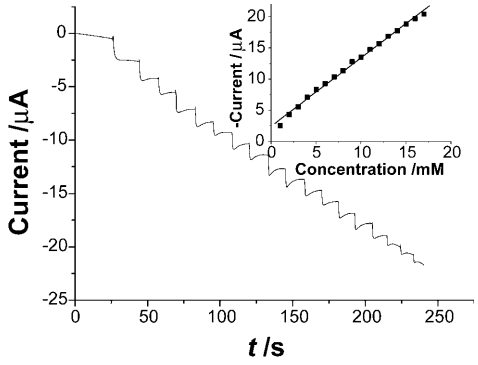

Figure 7. Response of the current–time curve of the GOx modified solid gold nanowire array electrode to successive additions of 1 mM glucose at −0.1 V in 0.1 M PBS. The upper right inset shows the calibration curve of the GOx-modified gold nanowire-array electrode toward glucose.

array electrodes have larger active surface area and allow larger quantities of enzyme to be immobilized and more efficient mass and electron transport to and from the enzyme sites compared to nonporous gold electrodes.

3. Conclusions

Porous gold nanowire arrays have been successfully fabricated within close-packed nanochannel alumina templates by one-step electrodeposition. The morphology of gold nanowires has a strong dependence on the current density, and the transformation from solid nanowire to porous nanowire can be realized by adjusting the current density. A glucose biosensor based on the GOx-modified porous Au nanowire arrays shows good analytical performance and can be reliably used for the detection of glucose. The method presented here is fast and inexpensive and may be extended to the fabrication of other oxidase-modified electrochemical biosensors.

Experimental Section

Glucose oxidase (GOx, from *Aspergillus niger*, 151 units mg^{-1}) and D-(+)-glucose were supplied by Sigma-Aldrich (Australia). All chemical reagents in this study were of analytical grade. A 1 M stock solution of glucose, prepared with distilled water, was left overnight at room temperature to allow equilibration of the anomers and then stored at 4 °C. Phosphate buffer solution (PBS, 0.1 M, pH 7) was prepared with Na_2HPO_4 and NaH_2PO_4 as electrolytes. All electrochemical depositions and electrochemical measurements were carried out on an electroanalytical instrument (autolab II) at room temperature. The enzyme electrode was used as working electrode, and a circular area (4 mm diameter) was exposed to the electrolyte. A KCl-saturated Ag/AgCl electrode was used as reference electrode, and a Pt foil as counterelectrode. Electrochemical impedance spectra were recorded in the frequency range between 10 kHz and 100 MHz at a formal potential of 200 mV and with sinusoidal modulation of amplitude of 10 mV rms. The morphology and microstructure of the Au nanowires were investigated with a scanning electron microscope (SEM, JEOL JSM-6300F) and a transmission electron microscope (TEM, Philips CM20).

The NCA templates were prepared by anodizing high-purity aluminum foils (99.999%) in oxalic acid solutions in a two-step anodization method.[47,48] NCA templates with selectable diameters, densities, and lengths can be formed by varying anodizing conditions. After anodization, the remaining aluminum was removed in saturated $HgCl_2$ solution. Subsequently, the pore bottoms were opened by chemical etching in 5 wt% phosphoric acid. NCA templates with pore diameters of about 65 nm were used to synthesize Au nanowires. To electrodeposit Au, an Au thin film was deposited on the back side of the anodic porous alumina template as electrode by using a vacuum evaporation apparatus. Electrodeposition was carried out by a galvanostatic method from the following solution: 12 g L^{-1} $HAuCl_4$, 160 g L^{-1} Na_2SO_3, 5 g L^{-1} ethylenediaminetetraacetic acid, 30 g L^{-1} K_2HPO_4, 0.5 g L^{-1} $CoSO_4$, pH 9.0. Unless otherwise noted, the cathode current density was kept at 10 $\mu A\,cm^{-2}$. The template was etched away by using 5 wt% phosphoric acid to release the gold nanowires. The obtained porous gold nanowire arrays were cleaned with 2 M HNO_3, ultrapure Millipore water, and ethanol. 0.15 g of GOx was added to 20 mL of PBS (0.1 M, pH 7) to prepare the GOx solution. The enzyme electrode was fabricated by immersing the porous gold nanowire-array electrode in the GOx solution for one day at 4 °C. GOx-modified solid gold nanowire-array electrodes were also prepared by the same method. The enzyme electrodes were washed and stored in PBS at 4 °C.

Acknowledgements

This work was supported by the Australian Research Council (DP0773160). X.Z. thanks the Australian Research Council for the Australian Research Fellowship.

Keywords: biosensors · electrochemistry · gold · nanostructures · template synthesis

[1] S. Iijima, *Nature* **1991**, *354*, 56.
[2] G. L. Che, B. B. Lakshmi, E. R. Fisher, C. R. Martin, *Nature* **1998**, *393*, 346.
[3] Z. D. Xiao, L. D. Zhang, X. K. Tian, X. S. Fang, *Nanotechnology* **2005**, *16*, 2647.
[4] Y. G. Li, B. Tan, Y. Y. Wu, *Nano Lett.* **2008**, *8*, 265.
[5] A. Yamaguchi, F. Uejo, T. Yoda, T. Uchida, Y. Tanamura, T. Yamashita, N. Teramae, *Nat. Mater.* **2004**, *3*, 337.
[6] Y. Y. Wu, T. Livneh, Y. X. Zhang, G. S. Cheng, J. F. Wang, J. Tang, M. Moskovits, G. D. Stucky, *Nano Lett.* **2004**, *4*, 2337.
[7] Y. G. Sun, Z. L. Tao, J. Chen, T. Herricks, Y. N. Xia, *J. Am. Chem. Soc.* **2004**, *126*, 5940.
[8] Y. L. Wang, X. C. Jiang, Y. N. Xia, *J. Am. Chem. Soc.* **2003**, *125*, 16176.
[9] C. R. Martin, *Science* **1994**, *266*, 1961.
[10] J. Li, C. Papadopoulos, J. M. Xu, M. Moskovits, *Appl. Phys. Lett.* **1999**, *75*, 367.
[11] E. Katz, I. Willner, *ChemPhysChem* **2004**, *5*, 1084.
[12] Y. Y. Wu, G. S. Cheng, K. Katsov, S. W. Sides, J. F. Wang, J. Tang, G. H. Fredrickson, M. Moskovits, G. D. Stucky, *Nat. Mater.* **2004**, *3*, 816.
[13] W. W. Yang, J. X. Wang, S. Zhao, Y. Y. Sun, C. Q. Sun, *Electrochem. Commun.* **2006**, *8*, 665.
[14] M. H. Yang, J. H. Jiang, Y. H. Lu, Y. He, G. L. Shen, R. Q. Yu, *Biomaterials* **2007**, *28*, 3408.
[15] K. B. Kokoh, J. M. Léger, B. Beden, C. Lamy, *Electrochim. Acta* **1992**, *37*, 1333.
[16] Y. Ling, J. C. Elkenbracht, W. F. Flanagan, B. D. Lichter, *J. Electrochem. Soc.* **1997**, *144*, 2689.
[17] F. L. Jia, C. F. Yu, K. J. Deng, L. Z. Zhang, *J. Phys. Chem. C* **2007**, *111*, 8424.
[18] F. L. Jia, C. F. Yu, Z. H. Ai, L. Z. Zhang, *Chem. Mater.* **2007**, *19*, 3648.
[19] Y. Y. Sun, F. Yan, W. S. Yang, C. Q. Sun, *Biomaterials* **2006**, *27*, 4042.
[20] J. Njagi, S. Andreescu, *Biosens. Bioelectron.* **2007**, *23*, 168.
[21] C. X. Ji, P. C. Searson, *J. Phys. Chem. B* **2003**, *107*, 4494.
[22] R. Laocharoensuk, S. Sattayasamitsathis, J. Burdick, P. Kanatharana, P. Thavarungkul, J. Wang, *ACS Nano* **2007**, *1*, 403.
[23] D. A. Gough, J. Y. Lucisano, P. H. S. Tse, *Anal. Chem.* **1985**, *57*, 2351.
[24] G. Fortier, D. Blanger, *Biotechnol. Bioeng.* **1991**, *37*, 854.
[25] B. Ballarin, C. J. Brumlik, D. R. Lawson, W. B. Liang, L. S. V. Dyke, C. R. Martin, *Anal. Chem.* **1992**, *64*, 2647.
[26] M. S. Celej, G. Rivas, *Electroanalysis* **1998**, *10*, 771.
[27] Y. H. Lin, F. Lu, Y. Tu, Z. F. Ren, *Nano Lett.* **2004**, *4*, 191.
[28] M. Gao, L. Dai, G. G. Wallace, *Synth. Met.* **2003**, *137*, 1393.
[29] E. Budevski, G. Staikov, W. J. Lorenz, *Electrochim. Acta* **2000**, *45*, 2559.
[30] A. K. M. Bantu, J. Rivas, G. Zaragoza, M. A. López-Quintela, M. C. Blanco, *J. Appl. Phys.* **2001**, *89*, 3393.
[31] X. Y. Zhang, L. D. Zhang, W. Chen, G. W. Meng, M. J. Zheng, L. X. Zhao, F. Phillipp, *Chem. Mater.* **2001**, *13*, 2511.
[32] T. Watanabe, S. Minami, *J. Jpn. Inst. Met.* **2000**, *64*, 67.
[33] T. Watanabe, *J. Jpn. Inst. Met.* **2002**, *66*, 339.
[34] M. Knichel, P. Heiduschka, W. Beck, G. Jung, W. Gpel, *Sens. Actuators B* **1995**, *28*, 85.
[35] E. Katz, I. Willner, *Electroanalysis* **2003**, *15*, 913.
[36] I. D. Raistrick, *Electrochim. Acta* **1990**, *35*,1579.

[37] H. K. Song, Y. H. Jung, K. H. Lee, L. H. Dao, *Electrochim. Acta* **1999**, *44*, 3513.
[38] J. P. Candy, P. Fouilloux, M. Keddam, H. Takenouti, *Electrochim. Acta* **1981**, *26*, 1029.
[39] K. A. Assiongbon, D. Roy, *Surf. Sci.* **2005**, *594*, 99.
[40] C. F. Yu, F. L. Jia, Z. H. Ai, L. Z. Zhang, *Chem. Mater.* **2007**, *19*, 6065.
[41] P. Forrer, F. Schlottig, H. Siegenthaler, M. Textor, *J. Appl. Electrochem.* **2000**, *30*, 533.
[42] J. Wang, *Chem. Rev.* **2008**, *108*, 814.
[43] J. Wang, J. Liu, L. Chen, F. Lu, *Anal. Chem.* **1994**, *66*, 3600.
[44] S. X. Zhang, W. W. Yang, Y. M. Niu, C. Q. Sun, *Anal. Chim. Acta* **2004**, *523*, 209.
[45] G. L. Long, J. D. Winefordner, *Anal. Chem.* **1983**, *55*, 713A.
[46] X. Zhang, J. Wang, B. Ogorevc, U. E. Spichiger, *Electroanalysis* **1999**, *11*, 945.
[47] H. Masuda, K. Fukuda, *Science* **1995**, *268*, 1466.
[48] H. Masuda, M. Staoh, *Jpn. J. Appl. Phys. Part 2* **1996**, *35*, L126.

Received: August 15, 2008
Revised: October 23, 2008
Published online on November 26, 2008

